

## Reactive Power Support to PV Grid System Using Voltage Source Converters to Enhance PV Penetration Level

Ramagiri Yerriswamy<sup>1</sup>, Dr.M.S Sujatha<sup>2</sup>

<sup>1</sup>(PG Scholar, EEE, Sree Vidyanikethan Engineering College, India)

<sup>2</sup>(Professor, EEE, Sree Vidyanikethan Engineering College, India)

---

**Abstract:** *In the distributed generation environment, existing standards impose limits on the allowable feeder voltage variation. These agreements must limit the power penetration level. If the penetration level increases it leads to increased or decreased feeder voltage and causes reverse current flow in the feeder. In order to mitigate this problem we need reactive power support to the feeder. By the use of conventional capacitor or inductor banks we cannot achieve full range of voltage control (voltage regulation).The work proposes a novel scheme containing auxiliary voltage source converter that enables the smooth tracking of reactive power according to the load requirement. The proposed system configuration can conveniently retrofit into the existing system within PV station itself and reliving the utility from additional voltage support burden. It in turns increases the PV penetration level in the feeder. The corresponding modeling, analysis and control design along with MATLAB Simulink results are discussed.*

**Keywords** - *Photovoltaic power systems, power system, reactive power control, stability, voltage profile, voltage source converter.*

---

### I. Introduction

Substantial and consistent rise in load demand has led to new strategies for maximizing the production of electricity, including the renewable energy sources such as wind, solar Photovoltaic (PV), tidal, etc. the solar PV-grid systems have gained importance in recent smart grid scenario because of their versatile characteristics and they have no environmental pollution, so penetration of PV-grid system in to power system is increasing as load demand increases.

Significant attention has been paid in recent times to the issues related to high PV power penetration and efforts have been made to mitigate the overvoltage (OV) and under-voltage (UV) problems because of the interface of widely varying power injection from photovoltaic sources and some of the present day loads have a very complex and unpredictable nature. This includes a big component of industrial loads which are reactive in nature. To reduce transmission losses and improve voltage profile, it is necessary to support at Least the reactive power demand through local generation [1], [2].

The principle owner of the incoming Distributed Generation System (DGS), e.g., PV-DGS expects maximum power and reliable generation from his system. In the foreseeable future, it is anticipated that the utility would expect the DGS client to support the power system with ancillary activities (e.g. power factor correction, dynamic stability, reactive power support, etc.) apart from injecting active power into the grid[3], [6]. Canova et al. [3], Liu et al. [4], and Steffel et al. [6] have reported that reverse power flow over a feeder is a major cause of voltage rise in power grid during high solar radiation. This limits the maximum PV penetration level into a given feeder which is determined by the bus voltage variation. Reactive power is a major influencing parameter in AC systems due to its impact on the line voltage profile. A dedicated Distribution Static Synchronous Compensator (D-STATCOM) at the Point of Common Coupling (PCC), for supplying reactive power demand and mitigating voltage variation in the area of dense disperse generation is a possible solution. Unfortunately this is not economical and having the following drawbacks [4]:

- 1) Reactive power can only be controlled in discrete steps due to which accurate voltage regulation is not possible.
- 2) Switching of inductive and capacitive banks may result in resonance.
- 3) Switching ON of capacitor can lead to severe voltage dip, followed by transients and switching OFF of inductor is associated with high transient recovery voltage issues.

Though the conventional method of reactive power compensation using D-STATCOM with discrete reactive power bank (RPB) is a feasible solution, it renders a poor dynamic performance of reactive power control due to the absence of feed forward compensation. Further, asynchronous discrete reactive power bank switching causes voltage transients. Moreover, a dedicate D-STATCOM may not be economical.

**The proposed systems have the following advantages [1]:**

- 1) The proposed system incorporates the STATCOM functionality through the PV inverter itself, without drastically increasing the latter's VA capacity. Dedicated STATCOM is obviated for reactive power compensation.
- 2) The scheme covers complete controllable range of reactive compensation smoothly (and not in discrete steps) despite using discrete banks. Hence, it can be used for precise voltage regulation.
- 3) The associated control scheme of the proposed system and analytically derived controllers ensure fast tracking response of the reactive power. Therefore, dynamic behavior of the system is improved substantially due to better controllability of reactive power compensation.
- 4) The increased reactive power capacity can be utilized for mitigating under and over voltages. This facilitates increased PV penetration level. Reactive power demand of local loads can be fed by the PV station, relieving the power system from reactive power support responsibility.

So the upcoming PV generating stations can be planned with existing reactive power banks such that the proposed scheme can be conveniently retrofitted into the existing systems with reactive power banks. The additional  $VSC_2$  used for synchronization is of much lower VA capacity as it is meant to supply only the power losses in the bank. This is expected to be an attractive and economical investment proposition to enhance the reactive power capacity of the station inverter.

## II. Proposed System Description And Operation

The proposed PV station configuration is shown in Fig. 1.  $VSC_1$  is the main PV-grid inverter, which may be a part of a single- or two-stage topology. The DC link voltage  $v_{DC}$  is controlled through  $VSC_1$ , therefore the PV generated power may be represented by an equivalent current source  $i_{MP}$ . An L-C filter is used for coupling of  $VSC_1$  with the grid. Fixed value capacitor bank ( $C_P$ ) and inductor bank ( $L_P$ ) are used with their breakers  $S_1$  and  $S_2$  to provide bulk reactive power support. The auxiliary converter  $VSC_2$  is used with reactive power banks to regulate the latter's voltages equal to the grid voltage by drawing power from the DC link or PV source, while switch  $S$  is open. The active power drawn by  $VSC_2$  to regulate its AC Output voltage is not significant because it only needs to feed the losses in the auxiliary network, including the inductor-capacitor bank. The reactive power capacity of both  $C_P$  and  $L_P$  banks are considered equal. The control strategy incorporated for  $VSC_1$  also handles the operation of switches  $S, S_1, S_2$  and  $S_3$ . The low power rheostat  $R_P$ , is required for momentary changeover of the switches, across  $L_P$  bank.

The proposed new system configuration includes the switching operation of the Reactive Power Banks (RPB) is integrated with the control scheme of the main PV voltage source inverter ( $VSC_1$ ) to generate controlled reactive power over the entire range. Any deficit reactive power requirement of local Electric Power System (EPS) is supplied by RPB. Transient issues, which might arise due to incompatibility of line and bank terminal voltages, are overcome by the auxiliary voltage source converter ( $VSC_2$ ).  $VSC_1$  is the main PV-grid inverter, which may be a part of a single- or two-stage topology. The DC link voltage  $V_{DC}$  is controlled through  $VSC_1$ , therefore the PV generated power may be represented by an equivalent current source  $i_{MP}$ . A  $L - C$  filter is used for coupling of  $VSC_1$  with the grid. Fixed value capacitor bank and inductor bank are used with their breakers and to provide bulk reactive power support [1]. The auxiliary converter is used with reactive power banks to regulate the latter's voltages equal to the grid voltage by drawing power from the DC link or PV source, while switch  $S$  is open. The active power drawn by  $VSC_2$  to regulate its AC output voltage is not significant because it only needs to feed the losses in the auxiliary network, including the inductor-capacitor bank. The reactive power capacity of both  $C_P$  and  $L_P$  banks are considered equal. The control strategy incorporated for also handles the operation of switches  $S, S_1, S_2$  and  $S_3$ . The low power rheostat  $R_P$ , is required for momentary changeover of the switches, across  $L_P$  bank.

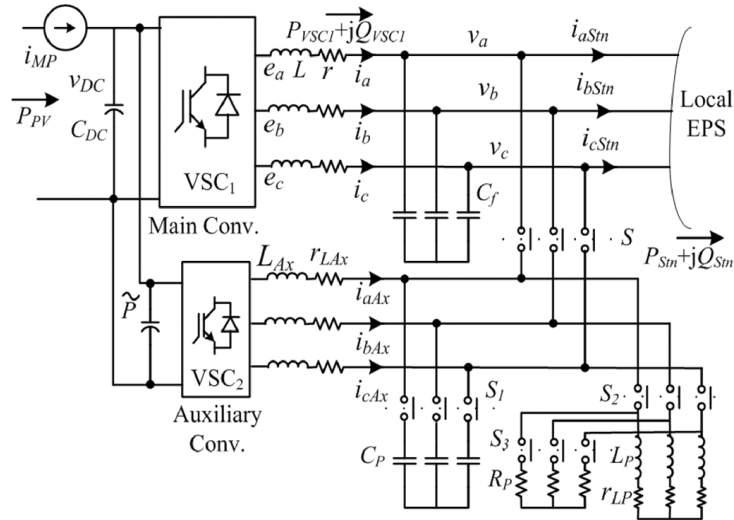


Fig.1. Proposed power circuit of PV-DGS with auxiliary converter and RPB [1]

The reactive power  $Q_{VSC1}$  injected  $VSC_1$  by serves as feedback for controlling switches  $S, S_1, S_2,$  and  $S_3$ . The operation of the proposed power circuit is represented by a state machine diagram in Fig. 2 that shows the sequence of control steps for all possible conditions. In conjunction with the system ensures smooth coupling of the RPBs with the grid under various conditions and facilitate complete control of the reactive power supplied by the station ( $Q_{stn}$ ). System is so designed that the reactive power capacity of  $VSC_1$  is at least half the individual capacity of  $C_P$  or  $L_P$  bank [4].

The sequence control of  $VSC_1, VSC_2$  and the various switches, as the operating conditions change, is as shown in Fig. 2 and follows:

- 1) During Low  $Q_{stn}$  demand:  $S$  is open;  $S_1$  and  $S_2$  are close;  $S_3$  is open;  $VSC_2$  is activated (for synchronization);  $VSC_1$  controls and meets the reactive power demand ( $Q_{stn} = Q_{VSC1}$ ).
- 2) Under condition (1), if  $Q_{stn}$  demand increases: then  $VSC_1$  contribution increases and hits the upper limit of  $+Q_{maxVSC1} \rightarrow VSC_2$  off  $S$  close;  $S_2$  close;  $S_2$  open.  $VSC_1$  Now controls surplus or deficit reactive power in addition to the capacitor ( $C_P$ ) reactive power ( $Q_{stn} = Q_{VSC1} + Q_{Cp}$ ).
- 3) When  $+Q_{stn}$  demand increases following condition:  $VSC_1$  contributes  $-Q_{VSC1}$  and hits the lower limit  $-Q_{maxVSC1} \rightarrow S$  is open  $S_2$  close and  $S_3$  open;  $VSC_2$  active and,  $VSC_1$  controls reactive power demand from station ( $Q_{stn} = Q_{VSC1}$ ).
- 4) When  $-Q_{stn}$  demand decreases following condition (4):  $Q_{VSC1} \rightarrow +Q_{VSC1}$  and hits the upper limit of  $+Q_{maxVSC1} \rightarrow S_2$  close.  $S$  Open; close  $\rightarrow S_3$  open; on,  $VSC_1$  controls the reactive power demand from the station ( $Q_{stn} = Q_{VSC1}$ ).

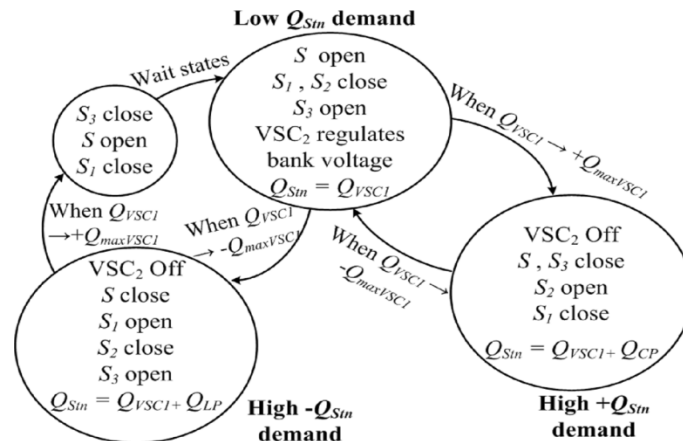


Fig 2. State machine diagram of the proposed reactive power enhancement scheme [1]

### III. Modelling and Controller Design

#### A. Current Controller Design for Main Inverter $VSC_1$ :

Both the inverters are controlled in the synchronously rotating reference frame. Indirect current control (applied to the inner current loop) is implemented by controlling the terminal voltages of the two inverters [9]. The PV inverter is grid tied voltage source inverter. Its DC link voltage is regulated by the outer voltage regulation loop with the active power component of current. Up on activation, maintains the voltage of RPB equal to grid voltage by outer AC voltage regulation [9]. The voltage at the grid side of the converter can be described as equation (1).

$$E_{abc} = L \frac{d}{dt} i_{abc} + v_{abc} + R i_{abc} \quad (1)$$

Where  $v_{abc}$  are converter input voltages, while  $i_{abc}$  are grid currents,  $E_{abc}$  are grid voltages,  $R$  and  $L$  are resistance and inductance respectively between the converter and the grid. Three-phase currents and voltages are transformed in  $dq$  reference frame by means of  $abc$  to  $dq$  transformation, where  $\omega$  is the system frequency in rad/s is given by (2).

$$\begin{bmatrix} E_d \\ E_q \end{bmatrix} = L \frac{d}{dt} \begin{bmatrix} i_d \\ i_q \end{bmatrix} + \omega L \begin{bmatrix} 0 & -1 \\ 1 & 0 \end{bmatrix} \begin{bmatrix} i_d \\ i_q \end{bmatrix} + R \begin{bmatrix} i_d \\ i_q \end{bmatrix} + \begin{bmatrix} v_d \\ v_q \end{bmatrix} \quad (2)$$

The governing circuit equations in synchronously rotating reference frame after segregating the components into real and imaginary parts can be written as equations (3) and (4) respectively.

$$\frac{di_d}{dt} = -\frac{r}{L} i_d + \omega_0 i_q + e_d - \frac{1}{L} v_d \quad (3)$$

$$\frac{di_q}{dt} = -\frac{r}{L} i_q - \omega_0 i_d + e_q - \frac{1}{L} v_q \quad (4)$$

Where  $v_d, v_q$  are the direct and quadrature components of the transformed grid voltages. If voltage vector is aligned with  $d$ -axis,  $v_q = 0, i_d, i_q$  are the current components,  $L$  and  $r$  are the filter elements of  $VSC_1$ . Where  $e_d, e_q$  are  $VSC_1$  generated voltage components with sinusoidal PWM switching technique.

$$e_d = \frac{V_{DC}}{2} m_d \quad e_q = \frac{V_{DC}}{2} m_q$$

$m_d, m_q$  are the modulation indexes

$$m_d = \frac{2}{V_{DC}} [u_d - L\omega_0 i_q + v_d]$$

$$m_q = \frac{2}{V_{DC}} [u_d + L\omega_0 i_q + v_q]$$

Assuming  $C_{DC}$  is large so  $V_{DC}$  link voltage may be considered as stable over the region of interest, so equations (3), (4) forms second order linear model of  $VSC_1$  with

$i_d, i_q \Rightarrow$  State variables

$m_d, m_q \Rightarrow$  control inputs

$v_d, v_q \Rightarrow$  Are used for the feed forward compensation

The transfer function can be obtained to design the inner current control loop is given by (5)

$$G_{i(s)} = \frac{I_d(s)}{U_d} = \frac{I_q(s)}{U_q} = \frac{1}{LS+r} \quad (5)$$

The transfer functions for controlling  $i_d, i_q$  are same with plant pole

$$LS + r = 0$$

$$S = -\frac{r}{L}$$

Since  $-\frac{r}{L}$  is very small plant pole is located close to the imaginary axis and effects the transient response of the current. PI controller is used to control the current components  $i_d, i_q$  with transfer function.

$$G(S) = \frac{K_p S + K_i}{S}$$

The location of the PI controller ‘zero’ is chosen such that  $\frac{K_i}{K_p} = \frac{r}{L}$  eliminates the plant pole and gives desired response. Loop transfer function is  $G_{i(s)} G_{ci(s)} = \frac{K_p}{Ls}$ .

Ideally, any band width can be achieved for the current control loop by adjusting  $K_p$ . But in practice, it is limited by the switching frequency ( $f_s$ ) of the converter. Thus  $\omega_{ci} = (1/10) \times (2\pi f_s)$ , where  $\omega_{ci}$  is the cut-off angular frequency thus, close loop transfer function of the current control loop,  $G_{CL}$  can be reduced to first order with unity gains given in (6):

$$G_{CL}(S) = \frac{1}{\frac{s}{\omega_{ci}} + 1} \quad (6)$$

$$K_p = L\omega_{ci} \text{ And } K_i = r\omega_{ci}$$

### B. Design of Dc Link Voltage Controller for $VSC_1$ :

Controllers for the inner current loops were designed assuming that  $V_{DC}$  is fairly constant during the reference current tracking operation. In practice, it is not possible to connect a very large capacitor at the DC link because firstly it is not economical and secondly a big capacitor will adversely affect the dynamic response of the DC link voltage [7]. The power balance condition across the DC and AC ports of the PV inverter can be used to model the DC link by expressing the capacitor voltage as a function of  $i_d$ ,  $P_{PV}$  (PV power output) and  $P_{loss}$  (inverter power loss)

$$P_{PV} = \frac{d}{dt} \frac{1}{2} C_{DC} V_{DC}^2 + P_{loss} + \frac{3}{2} v_d i_d \quad (7)$$

To avoid non-linearity,  $V_{DC}^2$  term can be considered as a state as well as an output variable of the plant model for the DC link voltage control. If  $P_{loss}$  is neglected it can be written as (8)

$$\frac{1}{2} C_{DC} \frac{d}{dt} V_{DC}^2 = P_{PV} - P_g = p \quad (8)$$

$P_g = \frac{3}{2} v_d i_d$  and  $p$  is a new control variable

Using (8), the transfer function for the DC link voltage control can be written as (9)

$$G_v = \frac{V_{DC}^2(S)}{p(S)} = \frac{2}{C_{DC} S} \quad (9)$$

The feed-forward compensation signal may be provided by the PV-Maximum Power Point Tracking (MPPT) [7]. The plant originally has a pole at origin, hence with additional integral term added to the controller so that the phase of loop transfer function is extended to  $-180^\circ$ .

A lead compensator is the best choice to provide a phase boost ( $\theta_{boost}$ ) at required  $\omega_{cutoff}$  of the gain plot. the DC link voltage controller  $G_{CV}$  has the following form

$$G_{CV}(s) = \frac{k s + \frac{r}{\alpha}}{s s + r}$$

Where  $r = \omega_{CV} \sqrt{\alpha}$

$$\alpha = \frac{1 + \sin\theta_{boost}}{1 - \sin\theta_{boost}}$$

### C. Current Controller for Auxiliary Inverter $VSC_2$ :

Though the primary responsibility of  $VSC_2$  is to regulate the AC terminal voltages of  $C_p$ , and  $L_p$  banks when the main switch  $s$  is off, the inner current control loop structure of  $VSC_2$  is same as that of  $VSC_1$ . Therefore (1) is still applicable and may be re-written for this case as follows:

$$L_{Ax} \frac{di_{dAx}}{dt} = -r_{Ax} i_{dAx} + L_{Ax} \omega_0 i_{qAx} + e_{dAx} - v_{dAx} \quad (10)$$

$$L_{Ax} \frac{di_{qAx}}{dt} = -r_{Ax} i_{qAx} + L_{Ax} \omega_0 i_{dAx} + e_{qAx} - v_{qAx} \quad (11)$$

The angular velocity of vectors is kept the same as that of  $VSC_1$  to achieve synchronous control of AC terminal voltages of  $C_p, L_p$  banks with grid terminal voltages.  $VSC_2$  shares the DC link with  $VSC_1$ . As the DC link voltage is regulated through  $VSC_1$ , the AC side variables of  $VSC_2$  can be independently controlled, assuming DC link voltage to be constant over the region of interest [7]. The bandwidth  $\omega_{CAUX}$  of the inner current control loop is chosen as

$$\omega_{CAUX} = (1/10) \times (2\pi f_{SAUX})$$

Where  $f_{SAUX}$  is the operating frequency of  $VSC_2$ .

The AC voltage control of the RPB (reactive power banks) using synchronous frame transformation represents 4<sup>th</sup> order control problem corresponding to  $d - q$  variables for  $C_p$  and  $L_p$  respectively shown in (14)

The vector differential equation corresponding to inductive RPB is as given in equations (12) and (13).

$$L_p \frac{di_{Lp}}{dt} = -r L_p i_{Lp} + v_{Ax} \tag{12}$$

and for capacitor bank

$$C_p \frac{dv_{Ax}}{dt} = i_{Ax} - i_{Lp} \tag{13}$$

The  $d - q$  components of the vectors can be segregated and represented in the state space form as in equation (14).

$$\begin{bmatrix} v_{dAx} \\ v_{qAx} \\ i_{dLp} \\ i_{qLp} \end{bmatrix} = \begin{bmatrix} 0 & \omega & \frac{-1}{C_p} & 0 \\ -\omega & 0 & 0 & \frac{1}{C_p} \\ \frac{1}{L_p} & 0 & \frac{-rL_p}{L_p} & \omega \\ 0 & \frac{1}{L_p} & -\omega & \frac{-rL_p}{L_p} \end{bmatrix} \begin{bmatrix} v_{dAx} \\ v_{qAx} \\ i_{dLp} \\ i_{qLp} \end{bmatrix} + \begin{bmatrix} \frac{1}{C_p} & 0 \\ 0 & \frac{1}{C_p} \\ 0 & 0 \\ 0 & 0 \end{bmatrix} \tag{14}$$

#### D. Compensator Design for PV Station Reactive Power:

The reactive power generation by the PV station is the combined response of the latter's inner current control (sitting in the control loop of reactive power component of current) and that of capacitive RPB (whenever switch is closed). This may be represented by the following non-linear equation (15) [using as a switch function S (1, 0)]

$$i_{qstn} = i_q + S[i_{qcp}] + i_{qcf} \tag{15}$$

The response of the inner reactive power component of the main inverter  $VSC_1$  is governed by equation (16) (17)

$$G_{CL}(S) = \frac{1}{\frac{S}{\omega_{ci}} + 1} \tag{16}$$

Where  $i_{qcp} = -\omega_0 C_p v_d i_{qcf} = -\omega_0 C_f v_d$

The plant model can be written as

$$i_{qstn}(s) = \frac{1}{\frac{S}{\omega_{ci}} + 1} i_q^*(s) - S \omega_0 C_p v_d(s) - S \omega_0 C_f v_d(s) \tag{17}$$

is taken as N

$$\therefore \frac{i_{qstn}(s)}{N} = \frac{1}{\frac{S}{\omega_{ci}} + 1}$$

∴ PI controller with feed forward compensation is found to be stable

$$K_p = \frac{\omega_{cstn}}{\omega_{ci}} \quad K_i = \omega_{cstn}$$

### IV. Results

The simulation result shows the smooth tracking of reactive power and Transient performance highlighting seamless interface during of RPB.

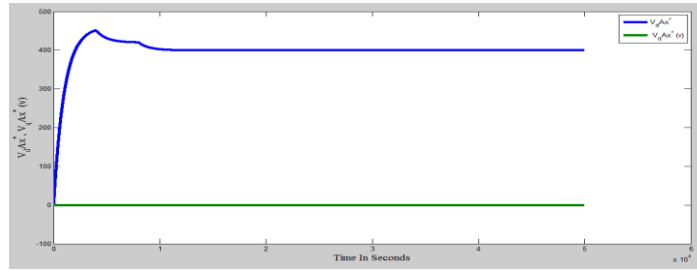


Fig.3 (a)

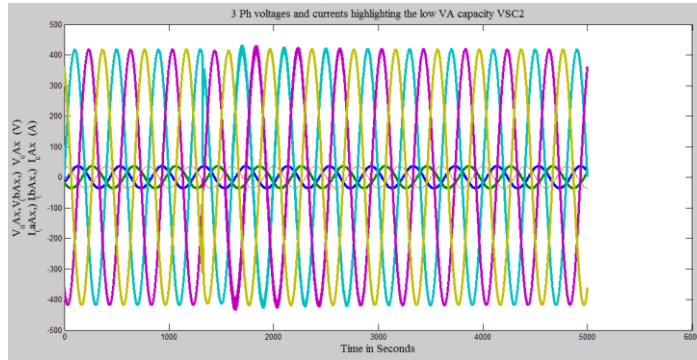


Fig.3 (b)

Fig.3. (a) Tracking performance of the  $d - q$  components of terminal voltage of RPB. (b) 3-Ph voltages and currents highlighting the low VA capacity.

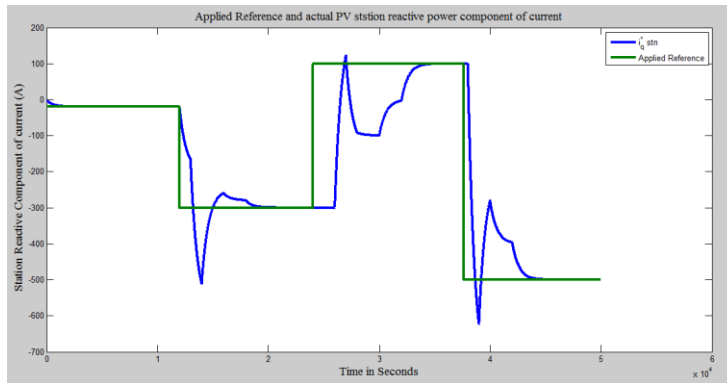


Fig.4(a)

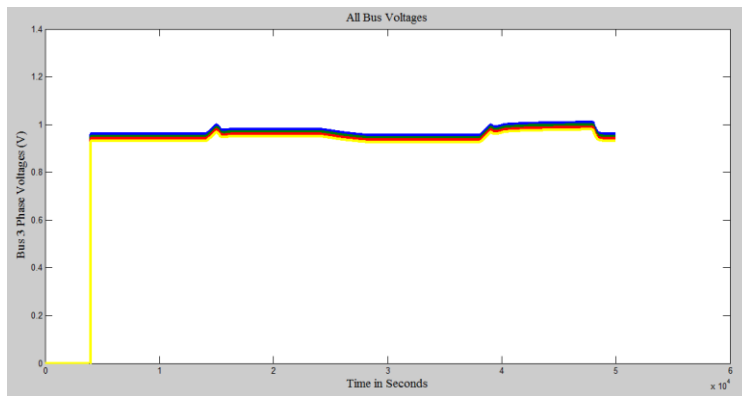


Fig.4(b)

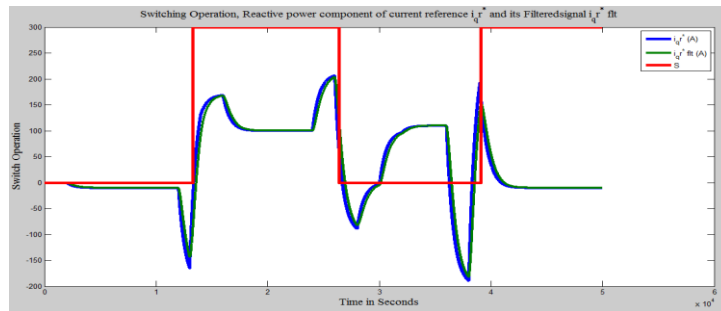


Fig.4(c)

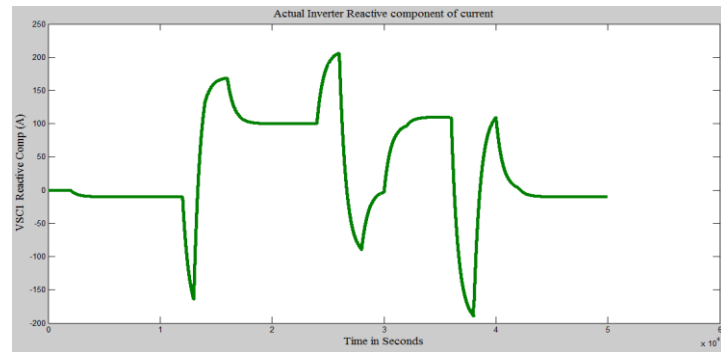


Fig.4(d)

**Fig. 4** PV station reactive power control performance. (a) Applied reference and actual PV station reactive power component of current. (b) All bus voltages. (c) Switch operation, reactive power component of current reference and its filtered signal. (d) Obtained reference and actual inverter reactive power component of current.

## V. Conclusion

Distributed power generation is being increased for reducing the stress on the power grid. The future power grid is likely to be with a large number of inverter driven DGS units. In addition to local power generation, it would be highly desirable to have these DGS units also compensate reactive power. The proposed scheme has demonstrated a viable method of enhancing the reactive power capacity of the inverter based DGS. The conventional methods of compensation based on discrete L-C banks have detrimental effects on the waveforms of feeder voltage and its regulation. The proposed scheme has addressed these issues by eliminating switching transients and providing full range of reactive power control. A notable feature of this scheme is that it can be conveniently retrofitted into the existing systems with reactive power banks.

## References

- [1] Rupesh.G. Wandhare, Vivek Agarwal, "Reactive power capacity enhancement of a PV-grid system to increase PV penetration level in smart grid scenario", *IEEE Trans. Smart grid*, vol. 5, no. 4, July 2014.
- [2] A. Di-Fazio, G. Fusco, and M. Russo, "Decentralized control of distributed generation for voltage profile optimization in smart feeders," *IEEE Trans. Smart Grid*, vol. 4, no. 3, pp. 1586–1596, Sep. 2013.
- [3] A. Rueda-Media and A. Padilha-Feltrin, "Distributed generators as providers of reactive power support-A market approach," *IEEE Trans. Power Syst.*, vol. 28, no. 1, pp. 490–502, Feb. 2013.
- [4] C. Chen, C. Lin, W. Hsieh, C. Hsu, and T. Ku, "Enhancement of PV penetration with DSTATCOM in Taipower distribution system," *IEEE Trans. Power Syst.*, vol. 28, no. 2, pp. 1560–1567, May 2013.
- [5] H. Sugihara, K. Yokoyama, O. Saeki, K. Tsuji, and T. Funaki, "Economic and efficient voltage management using customer-owned energy storage systems in a distribution network with high penetration of photovoltaic systems," *IEEE Trans. Power Syst.*, vol. 28, no. 1, pp. 102–111, Feb. 2013.
- [6] X. Liu, A. Aichhorn, L. Liu, and H. Li, "Coordinated control of distributed energy storage system with tap changer transformers for voltage rise mitigation under high photovoltaic penetration," *IEEE Trans. Smart Grid*, vol. 3, no. 2, pp. 897–906, Jun. 2012.
- [7] R. Tonkoski, D. Turcotte, and T. El-Fouly, "Impact of high PV penetration on voltage profiles in residential neighborhoods," *IEEE Trans. Sustain. Energy*, vol. 3, no. 3, pp. 518–527, Jul. 2012.
- [8] S. Steffel, P. Caroselli, A. Dinkel, J. Liu, R. Sackey, and N. Vadhar, "Integrating solar generation on the electric distribution grid," *IEEE Trans. Smart Grid*, vol. 3, no. 2, pp. 878–886, Jun. 2012.
- [9] C. Lin, W. Hsieh, C. Chen, C. Hsu, and T. Ku, "Optimization of photovoltaic penetration in distribution systems considering annual duration curve of solar Irradiation," *IEEE Trans. Power Syst.*, vol. 27, no. 2, pp. 1090–1097, May 2012.